B(Cl) respectively become $1\cdot85 \pm 0\cdot14$ and $1\cdot40 \pm 0\cdot08$ Å^2 for measurement No. 1 and $1\cdot75 \pm 0\cdot11$ and $1\cdot33 \pm 0\cdot06$ Å^2 for measurement No. 2. The corresponding values of R become 0·043 for measurement No. 1 and 0·049 for measurement No. 2. It is considered that use of β-filters only, together with fixed counter apertures, results in systematic deviations in the intensity measurements. The F_{meas} in Tables 2 and 4 should hence be regarded as illustrative of the evaluation method, and not as error-free data.

In summary, it is suggested that the criteria developed in this paper be applied to each diffractometer system built. Analysis of the results thus obtained should enable us to evaluate each system, not only in comparison with other systems, but also on an absolute basis.

It is a pleasure to thank J. L. Bernstein for his careful operation of PEXRAD and for the many computations performed on the IBM 7090.

References

ABRAHAMS, S. C. (1963). *Chem. Engng News*, **41**, 108.

ABRAHAMS, S. C. (1962*a*). ACA Meeting, Paper I–3, Villanova, Pa.

ABRAHAMS, S. C. (1962*b*). *Rev. Sci. Instrum.* **33**, 973.

ABRAHAMS, S. C. & BERNSTEIN, J. L. (1964). To be published.

BURBANK, R. D. (1961). *Rev. Sci. Instrum.* **32**, 368.

BURBANK, R. D. (1964). *Acta Cryst.* **17**, 434.

CETLIN, B. B. & ABRAHAMS, S. C. (1963). *Acta Cryst.* **16**, 943.

International Tables for X-ray Crystallography (1962). Vol. III, 202, 240. Birmingham: Kynoch Press.

LADELL, J. & SPIELBERG, N. (1964). To be published.

MURRAY, R. B. & MANNING, J. J. (1960). *IRE Trans. Nucl. Sc.* NS **7**: 2–3, 80.

PARRISH, W. (1962). *Advances in X-ray Diffractometry and X-ray Spectorgraphy*. Eindhoven: Centrex.

PATTERSON, A. L. (1962). Private communication.

SHORT, M. A. (1960). *Rev. Sci. Instrum.* **31**, 618.

Acta Cryst. (1964). **17**, 1195

Single-Crystal Diffractometry: The Improvement of Accuracy in Intensity Measurements

BY LEROY E. ALEXANDER AND GORDON S. SMITH

Mellon Institute, Pittsburgh 13, *Pennsylvania, U.S.A.*

(*Received* 13 *September* 1963)

Some important experimental factors are considered which must be chosen so as to satisfy a valid concept of integrated reflection intensity when using an incident X-ray beam taken directly off the target of the X-ray tube. The general superiority of the 2θ scan over the ω scan is demonstrated by an analysis of pertinent factors. A basic reason is that spectral dispersion can be readily allowed for in the 2θ scan by proper choice of the scan range, whereas in the ω scan it must be accomplished by regulation of the receiving aperture. Thus the ω-scan technique demands excessively wide apertures at large θ's when β-filtered radiation is employed and over very large ranges of θ when balanced filters are used. Very feeble reflections can often be measured more accurately by taking peak (I_p) rather than integrated (I_i) intensities, but such I_p data must be transformed into the equivalent I_i's by means of empirical correction curves for the crystal concerned. Other practical recommendations are made, and the results of five structure refinements are presented to illustrate the efficacy of the 2θ-scan technique.

1. Introduction

The success of diffractometric intensity measurements depends upon adherence to a valid working concept of integrated reflection intensity, $I_i(hkl)$. When the incident beam is taken directly off the target of the X-ray tube, a satisfactory concept can be based upon the experimental requirement that every point on the crystal be enabled to 'view' every point on the focal spot. It follows that when a crystal of negligible absorption is turned through the angular reflecting range of a set of planes (hkl) corresponding to a characteristic wavelength λ_0, every volume element contributes with equal weight to the overall (integrated) reflection intensity.

The present paper is devoted to a consideration of the important experimental factors which make it possible to conform in actual practice to the above definition of I_i. A working concept based on crystal-monochromatized radiation is more difficult to define and is not proposed. We devote our attention to three- or four-circle diffractometers of the normal-beam

equatorial type (Furnas & Harker, 1955; Furnas, 1957; Wooster, 1963) and consider in particular the 2θ and ω scanning techniques, which are the two limiting modes of scan for the collection of intensity data with diffractometers. The arguments set forth earlier (Alexander & Smith, 1962, hereafter designated AS) for the general superiority of the 2θ scan will be strengthened by additional considerations. Unavoidably some reiteration of topics from the previous treatment will be required in the interests of comprehensiveness and clarity.

Of first importance are the interrelated matters of spectral dispersion and the application of wavelength filters and other aids, such as pulse-height discrimination, to the minimization of radiation of wavelengths other than the characteristic, λ_0. Closely allied is the problem of excluding 'extraneous' λ_0 radiation, including especially parasitic and thermal diffuse scatter. The consideration of these topics necessitates the proper specification of the receiving aperture dimensions, with the result that all four matters become inextricably mixed in the following treatment.

2. The 2θ scan

The 2θ scan follows a diametral row line in the reciprocal lattice (r.l.), as shown in Fig. 1, and scans progressively not only the r.l. nodes generated by the characteristic radiation but also the continuous radiation spectra associated with them. Hence a reflection (hkl) is observed superposed upon a background consisting of scatter due to (1) wavelengths in the vicinity of λ_0 in the continuous spectrum, (2) harmonic and other wavelengths dispersed by neighboring nodes in the same r.l. row line, (3) parasitic radiation, (4) atomic thermal motions, and (5) the Compton effect (refer to AS, Figs. 6–10). Components (1), (2), (3) and (5) can be removed from the measured integrated intensity $I_i(hkl)$ rather effectively by simply subtracting the measured background intensity I_b. This procedure is also partially successful in eliminating thermal diffuse scattering, but it is neither wholly nor systematically effective in this regard since thermal diffuse scattering tends to 'peak up' at the r.l. points and since its distribution about the r.l. points is, in general, not known for any given crystal. Ordinarily the background is measured routinely at the endpoints of the selected scan ranges; for example, refer to columns 2 and 3 of Table 2. However, modified procedures are called for when the true background contour is very uneven or lost to view, as sometimes occurs at small Bragg angles (see also the last paragraph of § 6).

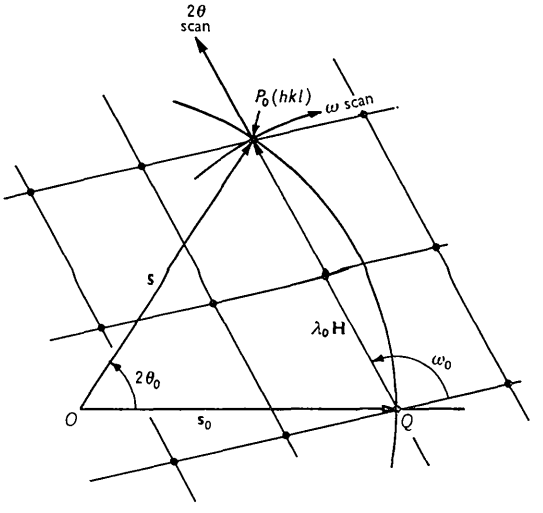

Fig. 1. Idealized reciprocal-lattice diagram of diffraction by planes (hkl) and measurement by the ω-scan and 2θ-scan techniques.

3. The ω scan

As explained previously (AS, pp. 985–6), an idealized ω scan may be visualized in terms of a perfect, point crystal and a point source of monochromatic X-rays, in which case the direction of scan is normal to a diametral r.l. row line as shown in Fig. 1. If now the row line also contains a continuous radiation 'streak' and if the receiving aperture has an angular width γ_R on the 2θ scale, the discrete intersection of the r.l. vector $\lambda_0\mathbf{H}(hkl)$ with the sphere of reflection at the diffraction angle $2\theta_0$ broadens into a short '2θ scan' along the r.l. row line extending from $\lambda_i\mathbf{H}$, through $\lambda_0\mathbf{H}$, to $\lambda_f\mathbf{H}$ as portrayed in Fig. 2. The limits of this scan are fixed by γ_R:

$$\gamma_R = 2\theta_f - 2\theta_i = 2\,[\sin^{-1}(\lambda_f H/2) - \sin^{-1}(\lambda_i H/2)]\,. \quad (1)$$

Referring to Fig. 2, for $\omega_f < \omega < \omega_i$ the scan in effect proceeds normal to the diametral r.l. row line, as in the ideal case, and enters the region of parasitic and thermal diffuse scatter lying between the row lines.

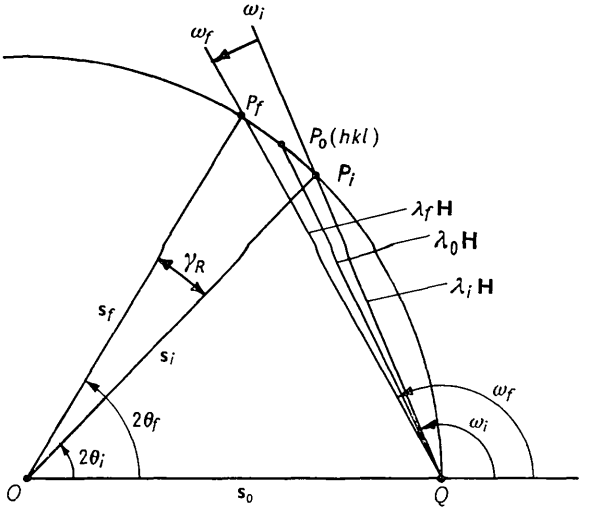

Fig. 2. Reciprocal-lattice geometry of the ω scan with receiving-aperture width γ_R.

Provided γ_R is sufficiently large, the ω scan is thus capable of revealing segments of the continuous radiation streak lying along the diametral row line on either side of the node (hkl). Under these conditions, just as in the 2θ scan, the intensity components (1), (2), (3) and (5) can be removed from the overall integrated reflection intensity by subtracting the background measured *on top of the general radiation streak*, say, at points b_1 and b_2 in Fig. 3(*a*). Although this method can be effective when judiciously applied (for example, Fischer & Hahn, 1961), it is subject to more or less serious errors if the receiving aperture

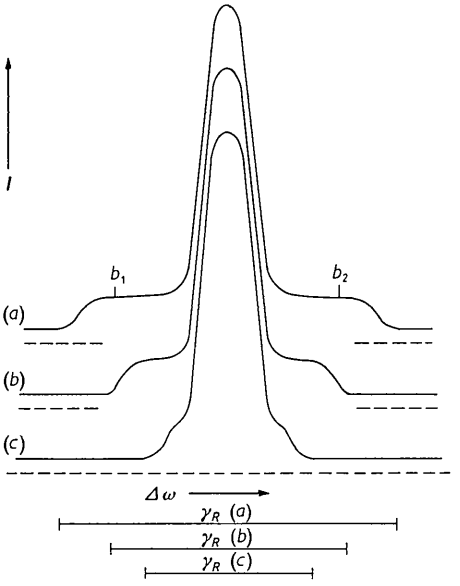

Fig. 3. Intensity profiles obtained by the ω-scan technique showing effects of (*a*) wide, (*b*) medium, (*c*) narrow receiving apertures.

is too narrow. Specifically, since the width of the reflection profile at small to moderate values of θ is principally due to the X-ray source, it is necessary that γ_R be not smaller than about $3\gamma_x$, γ_x being the overall angular width of the X-ray source profile. Thus for $\gamma_x = 0{\cdot}7°$, γ_R should certainly be no smaller than 2·0°. Figs. 3(*b*) and (*c*) illustrate the disappearance of the continuous radiation profile as γ_R is reduced.

Because of the tan θ dependence of spectral dispersion, at small Bragg angles the general radiation hump associated with a r.l. node (hkl) tends to contract within the main reflection profile and be lost to sight. This phenomenon is observable with either the 2θ or ω scan, and it is accentuated when γ_x and/or the direct lattice translations are large. Although in these circumstances the continuous-radiation background cannot be measured directly, a method of circumventing this difficulty when employing the 2θ-scan technique is described in § 7.

4. Use of Ross balanced filters

Subject to rather stringent limitations, Ross balanced filters (Ross, 1929), most effectively employed in conjunction with pulse-height discrimination, can be used with the ω scan to remove the contributions of extraneous wavelengths from the experimental values of $I_i(hkl)$. The first limitation is a consequence of the fact that spectral dispersion varies as tan θ. As a result, the angular width of the pass band, although practicably small at sufficiently small Bragg angles, tends to become prohibitively large as θ increases. Whereas in the 2θ scan spectral dispersion effects, including the pass band of a balanced-filter pair, can be encompassed by appropriately choosing the angular scan range, in the ω scan this can be accomplished only by adjusting the width of the receiving aperture. As Table 1 shows, for the relatively favorable case of the pair Zr and Y used with Mo radiation, the pass band range already exceeds 5° at $2\theta = 80°$, so that with the best scintillation counters currently available it is not feasible to make measurements above $2\theta = 60$ or 70°. For nearly all other balanced-filter pairs the angular widths of the pass bands at a given value of 2θ are much larger (Furnas, 1957, Table VII–2).

Table 1. *Angular pass bands* ($\Delta 2\theta$) *for balanced filters of* Zr *and* Y

2θ	$\Delta 2\theta$	K edge of Zr $2\theta_{min}$	K edge of Y $2\theta_{max}$
20°	1·10°	19·46°	20·56°
60	3·60	58·23	61·83
80	5·23	77·43	82·66
100	7·44	96·39	103·83

The second limitation on the use of Ross filters arises from the fact that parasitic and thermal diffuse scattering, being due very largely to $K\alpha$ radiation, are passed by the filter pair, as illustrated in Fig. 4. From the difference between the integrated intensities passed by the β and α filters it is necessary to determine and subtract the integrated intensity represented by the hatched zone of the figure. In order to do this it is necessary to make the four background measurements $(b_\beta)_1$, $(b_\beta)_2$, $(b_\alpha)_1$ and $(b_\alpha)_2$. This procedure is tedious in contrast to the simpler 2θ scan with two background measurements. When many hundreds or even some thousands of reflections are to be measured, as is to be expected for the majority of present-day structure determinations, the balanced-filter technique is not generally acceptable.

An additional weakness of the ω-scan-balanced-filter technique may be cited, namely, that the mandatory use of a wide receiving aperture at larger Bragg angles entails the reception of an unduly large amount of background scatter, which severely curtails

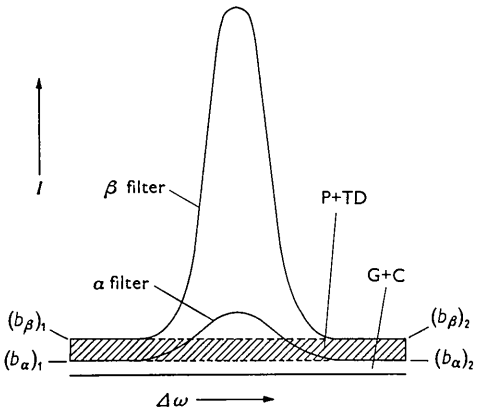

Fig. 4. Background intensity components transmitted by the α and β filters of a Ross balanced pair. The angular width of the filter pass band and γ_R are both larger than the range of $\Delta\omega$ shown. P+TD=parasitic plus thermal diffuse scatter. G+C=general radiation plus Compton scatter.

the accuracy with which weak reflections can be measured because of adverse counting statistics. In spite of the several deficiencies just described, the ω-scan-balanced-filter method has been employed successfully in studies by Young (1962) and by Verschoor & Keulen (1963).

5. Receiving aperture dimensions and scan range

The authors have previously given expressions (AS, Appendix D) for the vertical (or axial) and horizontal (or equatorial) dimensions of the receiving aperture. Although the correct choice of both dimensions is essential to the realization of valid intensity measurements, in the present treatment we confine ourselves to a discussion of the equatorial dimension. In defining the minimum width, $(\lambda_R)_{\min}$, pertinent to the ω scan with β filter, we shall at first neglect the requirement voiced in § 3 that $\gamma_R \geq 3\gamma_x$ in order to reveal adequately the continuous-radiation background. The values of $(\gamma_R)_{\min}$ appropriate to the 2θ and ω scans are then functions of the inherent reflecting range of the crystal (γ_m), spectral dispersion on the θ scale (γ_λ), angular diameter (γ_c) of the crystal subtended at the X-ray source, and angular width (γ_x) of the X-ray source subtended at the crystal. Recently the authors have revised the original expressions (Alexander & Smith, 1964) by incorporating more accurate terms in γ_c according to a suggestion of Burbank (1964). Most commonly the source-to-crystal distance is set equal to the crystal-to-receiver distance, in which case the equations reduce to:

$$2\theta \text{ scan, } (\gamma_R)_{\min}=2\gamma_m+\gamma_x+2\gamma_c \sin\theta . \quad (2)$$

$$\omega \text{ scan, } (\gamma_R)_{\min}=2\gamma_\lambda(\theta)+\gamma_x+2\gamma_c \cos\theta . \quad (3)$$

Of the four parameters only γ_λ is θ-dependent; it embodies two dispersion effects, both proportional to $\tan\theta$: dispersion within $K\alpha_1$ or $K\alpha_2$ and separation of $K\alpha_1$ and $K\alpha_2$. From these equations we see that spectral dispersion must be allowed for in the ω scan by proper choice of the receiving aperture width, whereas in the 2θ scan this is accomplished by adjustment of the scan range. The situation in this respect is entirely parallel to that discussed earlier involving the wavelength pass band of a balanced-filter pair.

The 2θ scan range may be appropriately set equal to the sum of two terms, the first a constant $(\Delta 2\theta)_0$ and the second proportional to $\tan\theta$, which is the term $2\gamma_\lambda(\theta)$ of equation (3). Now $(\Delta 2\theta)_0=2\gamma_m+2\gamma_x+2\gamma_c$, while $2\gamma_\lambda(\theta)$ is difficult to evaluate because of the indefinite angular width of the Cauchy-like spectral line profile. However, in practice it may be set equal to the angular separation of the $K\alpha$ doublet plus ten times the angular width of the $K\alpha_2$ line at half-maximum intensity.* This gives in degrees for Cu $K\alpha$ radiation $2\gamma_\lambda=0{\cdot}86\tan\theta$ and for Mo $K\alpha$ $1{\cdot}00\tan\theta$. Letting $2\gamma_m$, $2\gamma_x$, and $2\gamma_c$ have representative values of 0·3°, 1·4°, and 0·1° respectively, we obtain the following 2θ scan ranges:

$$\text{Cu } K\alpha, \ \Delta 2\theta=1{\cdot}80+0{\cdot}86\tan\theta \text{ degrees} . \quad (4)$$

$$\text{Mo } K\alpha, \ \Delta 2\theta=1{\cdot}80+1{\cdot}00\tan\theta \text{ degrees} . \quad (5)$$

From equation (3) the necessary receiving aperture widths for the ω-scan technique would be:

$$\text{Cu } K\alpha, \ (\gamma_R)_{\min}=0{\cdot}80+0{\cdot}86\tan\theta \text{ degrees} . \quad (6)$$

$$\text{Mo } K\alpha, \ (\gamma_R)_{\min}=0{\cdot}80+1{\cdot}00\tan\theta \text{ degrees} . \quad (7)$$

In equations (6) and (7) we have assigned to the term $2\gamma_c\cos\theta$ of equation (3) its fixed maximum value, $2\gamma_c$, since it is ordinarily very small in comparison with $2\gamma_\lambda+\gamma_x$.

Using the representative numerical parameters of equations (4) to (7), we give in columns 2, 3, 4 and 5 of Table 2 the required receiving aperture widths for the ω scan and 2θ scan ranges appropriate to Cu $K\alpha$ and Mo $K\alpha$ radiations for Bragg angles ranging from 10 to 80°. In practice it suffices to increase $\Delta 2\theta$ and $(\gamma_R)_{\min}$ stepwise over the experimental range of θ involved. An inspection of Table 2 shows that whereas it is possible to attain all the required 2θ-scan ranges in practice, the receiving apertures required in the ω-scan technique at large θ's are impossibly wide in the present stage of development of counters. Furthermore, even when realizable in experiment, the wider apertures called for in the table would sharply reduce the sensitivity of the apparatus to weak reflections, as was pointed out in connection with balanced filters.

To this point in the analysis of γ_R for the ω scan

* Previously the authors suggested five times the width of either $K\alpha$ component at half-maximum intensity (AS), but further consideration has shown a larger scan range to be desirable.

Table 2. *Minimum receiving aperture widths, $(\gamma_R)_{\min}$, for the ω-scan and minimum 2θ-scan ranges, $(\Delta 2\theta)_{\min}$, for typical experimental conditions*

$\gamma_m = 0{\cdot}15°$, $\gamma_x = 0{\cdot}7°$, $\gamma_c = 0{\cdot}05°$
$2\gamma_\lambda = 0{\cdot}86 \tan\theta$ and $1{\cdot}00 \tan\theta$ for Cu $K\alpha$ and Mo $K\alpha$ resp.

	$(\Delta 2\theta)_{\min}$ for 2θ scan (equations (4) and (5))		$(\gamma_R)_{\min}$ for ω scan (equations (6) and (7))		$(\gamma_R)_{\min}$ for ω scan (proper portrayal of background)	
θ	Cu $K\alpha$	Mo $K\alpha$	Cu $K\alpha$	Mo $K\alpha$	Cu $K\alpha$	Mo $K\alpha$
10°	1·95°	1·98°	0·95°	0·98°	2·00°	2·00°
20	2·11	2·16	1·11	1·16	2·00	2·00
30	2·30	2·38	1·30	1·38	2·00	2·00
40	2·52	2·64	1·52	1·64	2·00	2·00
50	2·83	2·99	1·83	1·99	2·00	2·00
60	3·30	3·53	2·30	2·53	2·30	2·53
70	4·17	4·55	3·17	3·55	3·17	3·55
80	6·70	7·47	5·70	6·47	5·70	6·47
(1)	(2)	(3)	(4)	(5)	(6)	(7)

we have ignored the constraint $\gamma_R \geq 3\gamma_x$ imposed by the need to portray the background properly. If this practical consideration is now allowed to take precedence in the calculation of the numerical values of Table 2, columns 4 and 5 must be replaced by 6 and 7, in which γ_R never assumes values less than 2°. The absence of a γ_m term in equation (3) discloses one circumstance apparently favorable to the ω scan, namely, its application to the measurement of a highly mosaic crystal. Nevertheless, even with γ_m as large as 1°, if we assign γ_x, γ_λ, and γ_c typical values of 0·7°, 0·2°, and 0·05° respectively, $(\gamma_R)_{\min}$ for the 2θ scan is 2·8°, whereas for the ω scan it is not less than 2·0° for the practical reason just explained. Certainly this is not a great disparity in favor of the ω scan. It is true that some alleviation would result for both the 2θ- and ω-scan techniques with β filtration if the X-ray source dimension were reduced. Other factors being favorable, however, it would probably be advantageous to measure the reflection intensities of such a highly mosaic crystal by the ω-scan-balanced-filter technique.

Table 3 summarizes the relative merits of three scanning techniques: (1) the 2θ scan with β filter, (2) the ω scan with β filter and $(\gamma_R)_{\min} = 3\gamma_x$, (3) the ω scan with balanced filters and $(\gamma_R)_{\min} = 2\gamma_\lambda + \gamma_x + 2\gamma_c$, where $2\gamma_\lambda$ is the angular width of the pass band on the 2θ scale. It is clear that on the basis of all the evidence examined, the 2θ scan is to be preferred for general use.

6. Integral versus peak intensities

The authors strongly recommend that in ordinary practice integrated intensities be measured directly, although in certain circumstances it may occasionally be advantageous to employ the stationary-crystal stationary-counter technique to measure peak intensities, $I_p(hkl)$. The measurement of very feeble reflections constitutes such a situation, because then I_p/I_b

Table 3. *Concise summary of the characteristics of the ω- and 2θ-scan techniques*

	2θ scan, β filter	ω scan, β filter, $(\gamma_R)_{\min} = 3\gamma_x$	ω scan, balanced filters, $(\gamma_R)_{\min} = 2\gamma_\lambda^* + \gamma_x + 2\gamma_c$
1. Number of measurements required	1 scan 2 backgrounds	1 scan 2 backgrounds	2 scans 4 backgrounds
2. Elimination of wavelengths other than λ_0 from net measured value of I_i	satisfactory	satisfactory except at large 2θ's	satisfactory within restricted 2θ range
3. Elimination of parasitic and Compton scatter	satisfactory	satisfactory	satisfactory
4. Elimination of thermal diffuse scatter	incomplete	incomplete	incomplete
5. Allowance for increase of spectral dispersion with θ	satisfactory except at large 2θ's	unsatisfactory in general	unsatisfactory in general
6. Effectiveness in measuring weak intensities	satisfactory	unsatisfactory	unsatisfactory
7. Suitability for highly mosaic crystals	unsatisfactory	satisfactory	satisfactory

* $2\gamma_\lambda$ = angular width of pass band on 2θ scale.

is appreciably larger than I_i/I_b, resulting in better resolution of the (*hkl*) peak from the background. The reader is reminded that the relative standard deviation in the net intensity (above background) of the (*hkl*) peak is given by

$$\sigma=(N_t+N_b)^{\frac{1}{2}}/(N_t-N_b)\,, \qquad (8)$$

where N_t and N_b are respectively the overall counts and background counts recorded (Klug & Alexander, 1954, p. 272). However, as the authors have previously emphasized (AS) concerning the 2θ scan, only in a limited low-2θ region is I_p approximately proportional to I_i, while at larger Bragg angles the ratio I_i/I_p increases rapidly to values exceeding 1·5 times its value at $2\theta \rightarrow 0°$. Because of variations in mosaic character from one crystal to another, it is not possible to rely upon any one calculated or experimental curve of I_i/I_p *versus* 2θ for the correction of I_p's to the equivalent I_i's, as an inspection of Fig. 5 will show. It is necessary to plot such curves directly from selected reliable reflections of the crystal concerned, making due allowance for the possible occurrence of anisotropy.

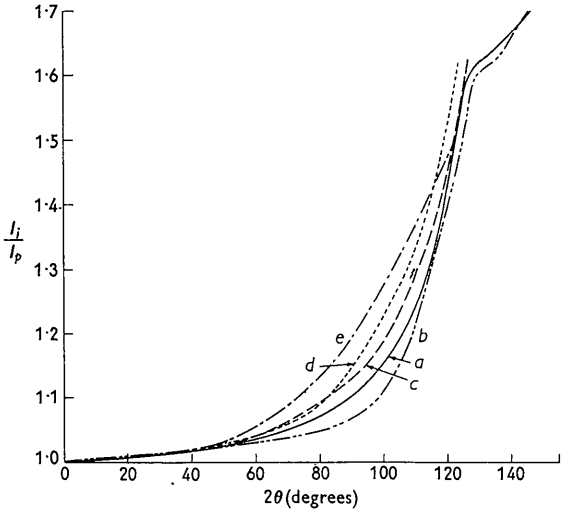

Fig. 5. Comparison of calculated and experimental curves of I_i/I_p for Cu $K\alpha$ radiation.
(*a*) Calculated, (*b*) α-quartz, (*c*) $(C_6H_5)_4Si$,
(*d*) cyclic tetramer $[(CH_3)_2SiNH]_4$,
(*e*) $(C_6H_5)_2SiCH_2CH_2Si(C_6H_5)_2$.
O

We wish to call renewed attention to a special value of the I_i/I_p curve which has been cited earlier (AS, p. 994) in connection with the shrinkage of the general radiation hump under the reflection profile at small θ's. Under such circumstances the proper value of the background is that which, when subtracted from the overall experimental values of I_i and I_p, will cause the ratio (I_i/I_p) for the reflection to fall on the previously established I_i/I_p correction curve of the crystal concerned.

7. Further practical recommendations

(1) Possible crystal specimens should be evaluated in advance by photographic and/or counter techniques for (*a*) mosaic character and (*b*) absorption and extinction properties. Item (*a*) furnishes the needed value of γ_m for the calculation of $(\gamma_R)_{\min}$ by equation (2) (Alexander, Smith & Brown, 1963). Item (*b*) involves the measurement of the variation in I_i for equivalent faces of a crystallographic form, and this information is useful as a criterion for acceptance of a given crystal or as an aid in assigning weights to the F_o's in the crystal structure analysis.

(2) When feasible in relation to other considerations, employ a short wavelength in order to minimize the number of intensity measurements to be performed in the high-2θ region.

(3) One must always be alert to the possible presence of uneven background contours, frequently the result of interference by a neighboring reflection. Such effects will be most pronounced when a short wavelength is employed and for crystals with large unit cells. For crystals with very large cells (for example, proteins) it is helpful to employ long-wavelength radiation and to reduce γ_x by adjusting the target 'take-off' angle in order to improve the resolution of densely populated r.l. row lines. Excessive loss of primary beam intensity imposes an ultimate limit on the minimum acceptable value of γ_x.

(4) In order to compensate for possible long-period variations in primary beam intensity and monotonic decline in the reflecting power of the crystal due to radiation damage or other causes, all measured $I_i(hkl)$ data should be referred to the intensity of a standard reflection measured at regular intervals (normally not less frequently than twice daily).

(5) When known to be significant, errors due to thermal diffuse scattering may be reduced, other considerations permitting, by reducing the temperature of the crystal during measurement.

(6) The accuracy of measurement of feeble reflections may be improved by (*a*) using a larger-than-average crystal, (*b*) minimizing parasitic scatter by careful experimental procedures and apparatus design, (*c*) carefully minimizing γ_R according to equation (2), (*d*) measurement of I_p and transformation to I_i by means of a correction curve.

8. Illustrative results

Table 4 summarizes the results of five structure refinements performed at Mellon Institute with diffractometric intensities collected by the procedures

Table 4. *Results of five structure refinements employing diffractometric intensities*

DS = differential synthesis LS = least squares IA = individual anisotropic II = individual isotropic

Crystal	α-quartz		GeO_2		$(C_6H_5)_4Si$	$(C_6H_5)_4Sn$	$[(H_3C)_2SiNH]_4$ cyclic
Radiation	Cu $K\alpha$		Mo $K\alpha$		Cu $K\alpha$	Mo $K\alpha$	Cu $K\alpha$ partial Mo $K\alpha$ partial
Method of refinement	DS and LS		LS		LS	LS	LS
Number of intensity data	112 (complete 3D)		194 (complete up to $2\theta \approx 68°$)		621 (complete 3D)	750 (partial) 350 $hk0$, $0kl$, and hhl 400 hkl	934 (partial) 639 $hk0$, $0kl$, and $h0l$ 295 hkl
Number of parameters							
Positional	4		4		33*	33*	48†
Thermal	10		10		68*	68*	16†
Kind of temperature factor	IA		IA		IA	IA	II
Final R(%)	DS	LS					
All F_o's	3·3	3·6	1·9	1·6‡	3·9	4·0	8·6
Non-zero F_o's	3·3	3·6	1·9	1·6‡	3·3	3·0	7·9

* Including H atoms. † H atoms not located. ‡ Extinction assumed for three reflections.

suggested in the present paper, which made use exclusively of β-filtered incident X-rays. As the criterion of excellence of structural refinement we have employed the conventional reliability index,

$$R = \Sigma(|F_o| - |F_c|)/\Sigma|F_o| \, .$$

References

ALEXANDER, L. E. & SMITH, G. S. (1962). *Acta Cryst.* **15**, 983.

ALEXANDER, L. E. & SMITH, G. S. (1964). *Acta Cryst.* **17**, 447.

ALEXANDER, L. E., SMITH, G. S. & BROWN, P. E. (1963). *Acta Cryst.* **16**, 773.

BURBANK, R. D. (1964). *Acta Cryst.* **17**, 434.

FISCHER, K. & HAHN, T. (1961). *Z. Kristallogr.* **116**, 27.

FURNAS, T. C. (1957). *Single Crystal Orienter Instruction Manual.* Milwaukee: General Electric Company.

FURNAS, T. C. & HARKER, D. (1955). *Rev. Sci. Instrum.* **26**, 449.

KLUG, H. P. & ALEXANDER, L. E. (1954). *X-ray Diffraction Procedures.* New York: Wiley.

ROSS, P. A. (1928). *J. Opt. Soc. Amer.* **16**, 433.

VERSCHOOR, A. C. & KEULEN, E. (1963). Private communication.

WOOSTER, W. A. (1963) *J. Sci. Instrum.* **40**, 14.

YOUNG, R. A. (1962). *Final Report*, Contract No. AF 49(638)–624, Project A–447, Georgia Institute of Technology, Atlanta, Ga.